

Scattering at the Anderson transition: Power-law banded random matrix model

J. A. Méndez-Bermúdez^{1,2,3} and I. Varga^{4,5}

¹*Max-Planck-Institut für Dynamik und Selbstorganisation, Bunsenstrasse 10, D-37073 Göttingen, Germany*

²*Department of Physics, Ben-Gurion University, Beer-Sheva 84105, Israel*

³*Instituto de Física, Universidad Autónoma de Puebla, Apartado Postal J-48, Puebla 72570, Mexico*

⁴*Elméleti Fizika Tanszék, Fizikai Intézet, Budapesti Műszaki és Gazdaságtudományi Egyetem, H-1521 Budapest, Hungary*

⁵*Fachbereich Physik und Wissenschaftliches Zentrum für Materialwissenschaften,*

Philipps Universität Marburg, D-35032 Marburg, Germany

(Dated: September 11, 2018)

We analyze the scattering properties of a periodic one-dimensional system at criticality represented by the so-called power-law banded random matrix model at the metal insulator transition. We focus on the scaling of Wigner delay times τ and resonance widths Γ . We found that the typical values of τ and Γ (calculated as the geometric mean) scale with the system size L as $\tau^{\text{typ}} \propto L^{D_1}$ and $\Gamma^{\text{typ}} \propto L^{-(2-D_2)}$, where D_1 is the information dimension and D_2 is the correlation dimension of eigenfunctions of the corresponding closed system.

PACS numbers: 03.65.Nk, 71.30.+h, 72.15.Rn, 73.23.-b,

I. INTRODUCTION

The investigation of the disorder induced metal-insulator transition (MIT) is an exciting and yet unsolved problem in condensed matter physics. During the past almost fifty years of research many important features have been cleared out using analytical, numerical, and experimental techniques. Yet this problem continues to bring interesting and unexpected novelties to daylight.^{1,2,3}

Many characteristics of disordered metals and those of insulators have been understood over the past. The spectral fluctuations of a disordered metal are well described by random matrix theory, while the fluctuations of a system in the insulating regime follow the Poisson statistics.^{4,5} The nature and the details of the MIT, on the other hand, still belong to the most intensively studied problems. We know already that the spectral fluctuations of a system right at the transition have properties merged from the two extremes.⁴ However, relations between the spectral and eigenfunction fluctuations show that there is an intimate connection between the two⁶ which is related to anomalous wave packet spreading and diffusion.⁷

Recently, several works have been devoted to deepen our understanding of the scattering properties of disordered systems by analyzing the distribution of resonance widths and Wigner delay times.^{8,9,10,11,12,13,14,16,17} Both distribution functions have been shown to be closely related to the properties of the corresponding closed system, i.e., the fractality of the eigenstates and the critical features of the MIT. In this respect, detailed analysis have been performed for the three-dimensional (3D) Anderson model¹⁴ and also for the power law band random matrix (PBRM) model.^{18,19,20,21,22,23} The PBRM model, which describes a one-dimensional (1D) sample with random long-range hopping, has been found to provide many of the features of the localization-delocalization transition present in the 3D Anderson model.

In the present work we look at the PBRM model more

closely to see how general are the findings presented in Refs. 8,14, and 17. Here, we find good scaling of the distribution functions of resonance widths and Wigner delay times. Moreover, we state new scaling relations of their typical values (i.e., their geometric mean) determined by the information dimension, D_1 , and the correlation dimension, D_2 , of the eigenfunctions of the corresponding closed system. We note that D_2 also governs the spreading of wave packets in systems at the MIT.⁷

Finally, we have to mention that in recent microwave experiments the study of systems in which the resonance states resemble the characteristics of those of our interest was reported.²⁴ Therefore the direct verification of our results is expected to be available in the near future.

The organization of this paper is as follows. In the next section we describe the model we use and define the scattering setup. Section III is devoted to the analysis of the coupling between sample and lead. In Sec. IV we present our results for the distribution functions of resonance widths and Wigner delay times. Finally, Sec. V is left for conclusions.

II. MODEL

The isolated sample of length L is represented by an $L \times L$ real symmetric matrix whose entries are randomly drawn from a normal distribution with zero mean, $\langle H_{ij} \rangle = 0$, and a variance depending on the distance of the matrix element from the diagonal as

$$\langle (H_{ij})^2 \rangle = \frac{1}{2} \frac{\delta_{ij} + 1}{1 + [\sin(\pi|i-j|/L)/(\pi b/L)]^{2\alpha}}, \quad (1)$$

where b and α are parameters. In order to reduce finite size effects this expression already incorporates periodic boundary conditions, where Eq. (1) is known as the periodic PBRM model. Nevertheless, for sites far away from each other and the border, i.e., $1 \ll |i-j| \ll N$, the

variance decays with a power law

$$\langle (H_{ij})^2 \rangle \sim \left(\frac{b}{|i-j|} \right)^{2\alpha}. \quad (2)$$

Field-theoretical considerations^{18,20,23} and detailed numerical investigations^{21,22} verified that the PBRM model undergoes a transition at $\alpha = 1$ from localized states for $\alpha > 1$ to delocalized states for $\alpha < 1$. This transition shows all the key features of the Anderson MIT, including multifractality of eigenfunctions and non-trivial spectral statistics at the critical point. At the center of the spectral-band a theoretical estimation for the multifractal dimensions, D_q , of the eigenfunction $\psi(\mathbf{r})$ gives¹⁹

$$D_q = \begin{cases} 4b\tilde{\Gamma}(q-1/2)[\sqrt{\pi}(q-1)\tilde{\Gamma}(q-1)]^{-1}, & b \ll 1 \\ 1 - q(2\pi b)^{-1}, & b \gg 1 \end{cases} \quad (3)$$

where $\tilde{\Gamma}$ is the Gamma function. D_q is defined through the Rényi entropy²⁵ of the participation number^{22,23,26,27}

$$\mathcal{R}_q = \frac{1}{1-q} \ln \mathcal{N}_q \propto D_q \ln L, \quad (4)$$

where the participation number is defined as

$$\mathcal{N}_q = \left(\int |\psi(\mathbf{r})|^{2q} d\mathbf{r} \right)^{-1} \quad (5)$$

showing a nontrivial scaling with respect to the linear size of the system L . Thus model (1) possesses a line of critical points $b \in (0, \infty)$, where the multifractal dimensions D_q change with b . The value of parameter b describes the strength of disorder. In other words it is related to the classical conductance through the relation²⁰ $g_c = 4\beta b$, where β stands for the global symmetry of the system: $\beta = 1$ describes the presence and $\beta = 2$ the absence of time reversal symmetry.

Among all dimensions, the information dimension D_1 and the correlation dimension D_2 play a prominent role.²⁸ However, D_1 is obtained as the $q \rightarrow 1$ limit of Eq. (4), being the scaling of the Shannon entropy.²⁸

We have to mention that recently a phenomenological formula was obtained in Ref. 29 for the exponent D_2 as a function of b (and in this way as a function of g_c):

$$D(b) = \frac{1}{1 + (\sigma b)^{-1}}, \quad (6)$$

where σ is a fitting parameter. For the present model we found that $\sigma \approx 2.85$ reproduces well the numerical D_2 extracted from \mathcal{N}_2 ,²² see Eq. (5). Similarly Eq. (6) fits well the exponent D_1 with $\sigma \approx 5.6$. See Fig. 1.

We turn the isolated system to a scattering one by attaching one semi-infinite single channel lead to it. The lead is described by the following 1D tight-binding Hamiltonian:

$$H_{\text{lead}} = \sum_{n=1}^{-\infty} (|n\rangle\langle n+1| + |n+1\rangle\langle n|). \quad (7)$$

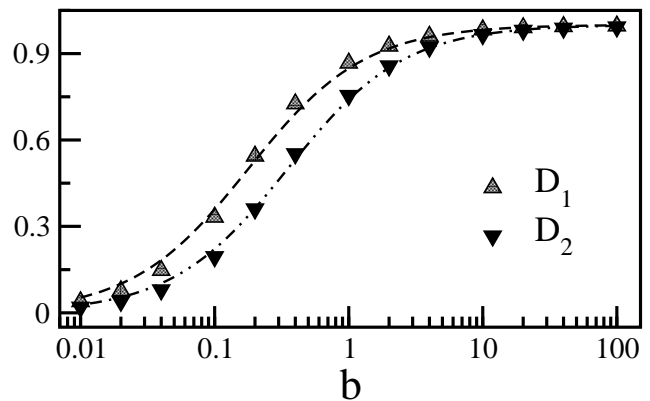


FIG. 1: D_1 and D_2 as a function of b . Lines correspond to Eq. (6) with $\sigma \approx 5.6$ (dashed) and $\sigma \approx 2.85$ (dot-dashed).

Using standard methods³⁰ one can write the scattering matrix (a single complex number for one attached lead) in the form^{14,16}

$$S(E) = e^{i\Phi(E)} = 1 - 2i\pi W^T (E\mathbf{1} - \mathcal{H}_{\text{eff}})^{-1} W, \quad (8)$$

where $\mathbf{1}$ is an $L \times L$ unit matrix and \mathcal{H}_{eff} is an effective non-hermitian Hamiltonian given by

$$\mathcal{H}_{\text{eff}} = H - i\pi W W^T. \quad (9)$$

Here, W is an $L \times 1$ vector with elements $W_n = w_0 \delta_{nn_0}$, where w_0 is the coupling strength between sample and lead and n_0 is the site at which the lead is attached. All our calculations take place in an energy window close to the band center ($E = 0$). Then, the Wigner delay time is given by^{14,16,31}

$$\tau(E=0) = \left. \frac{d\Phi(E)}{dE} \right|_{E=0} = -2\text{ImTr}(E - \mathcal{H}_{\text{eff}})^{-1} \Big|_{E=0}. \quad (10)$$

In addition to the delay times, which captures the time-dependent aspects of quantum scattering, the poles of the scattering matrix are also of great relevance.¹⁷ They determine the conductance fluctuations of a quantum dot in the Coulomb blockade regime³² or the current relaxation.³ The poles of the scattering matrix show up as resonances, which are the complex eigenvalues $\mathcal{E}_n = E_n - i\Gamma_n/2$ of \mathcal{H}_{eff} . E_n and Γ_n are the position and width of the n th resonance, respectively. Of course for $w_0 = 0$ the real part of the poles, E_n , correspond to the eigenvalues of the closed system. The Γ_n s, on the other hand, are related to the lifetime of the resonances through $\tau_n = 1/\Gamma_n$. Thus, we may expect close correspondence between Wigner delay times and the resonance widths which, in fact, we calculate independently from each other. Below we use matrices of sizes varying from $L = 50$ up to $L = 800$ to compute probability distribution functions of scattering phases Φ , Wigner delay

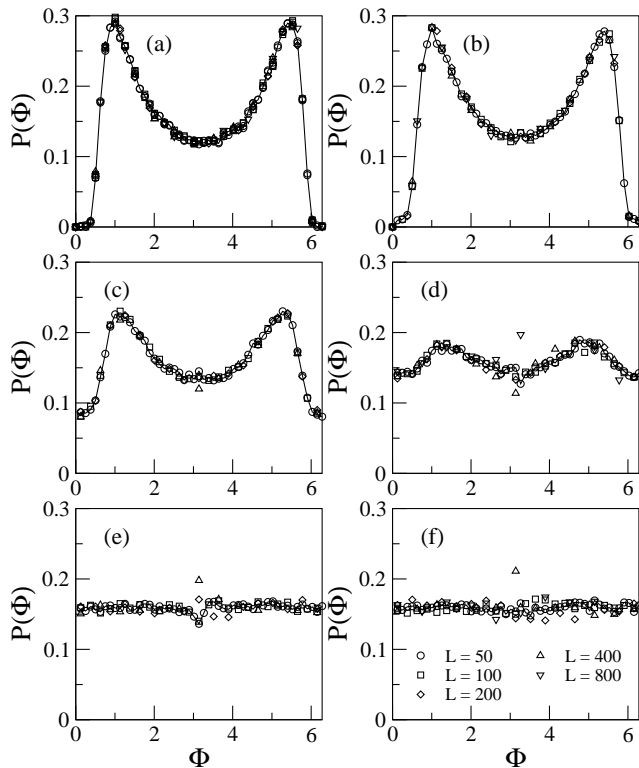


FIG. 2: $\mathcal{P}(\Phi)$ corresponding to w_0 where $|\langle S \rangle|$ takes its minimum value (perfect coupling condition) for (a) $b = 0.01$ and 0.04 , (b) $b = 0.1$, (c) $b = 0.4$, (d) $b = 1$, (e) $b = 4$, and (f) $b = 10$. We use (a) $w_0 = 0.6$, (b) $w_0 = 0.65$, (c) $w_0 = 0.9$, (d) $w_0 = 1.55$, and (e) $w_0 = 3.4$. In (f) $w_0 = 5.1$, $w_0 = 5.43$, and $w_0 = 5.5$ for $L = 50$, $L = 100$, and $L \geq 200$, respectively.

times τ , and resonance widths Γ . For statistical processing a large number of disorder realizations is used. In the case of $\mathcal{P}(\Phi)$ and $\mathcal{P}(\tau)$ we have at least 100000 data values. For the statistics of Γ we use the eigenvalues around $E_n \sim 0$, about one tenth of the total spectra. Here, at least 250000 data values are used.

III. PERFECT COUPLING

In this section we define more precisely the way the lead is attached to the system under the condition of perfect coupling. We should first note that the lead is attached to any site (chosen at random) within the sample and that the ensemble average also implies average over the position of the lead. The value of the coupling strength, w_0 , is defined by analyzing the distribution of the scattering phases $\mathcal{P}(\Phi)$. See also Ref. 8. In Fig. 2 we present $\mathcal{P}(\Phi)$ for various values of b and L . We use (here and below) the coupling strengths w_0 such that $|\langle S(w_0) \rangle| \approx 0$, where the corresponding setup is associated with perfect coupling between sample and lead. $\langle S \rangle$ is the ensemble average of the S matrix. Notice that for $b > 1$ we recover the uni-

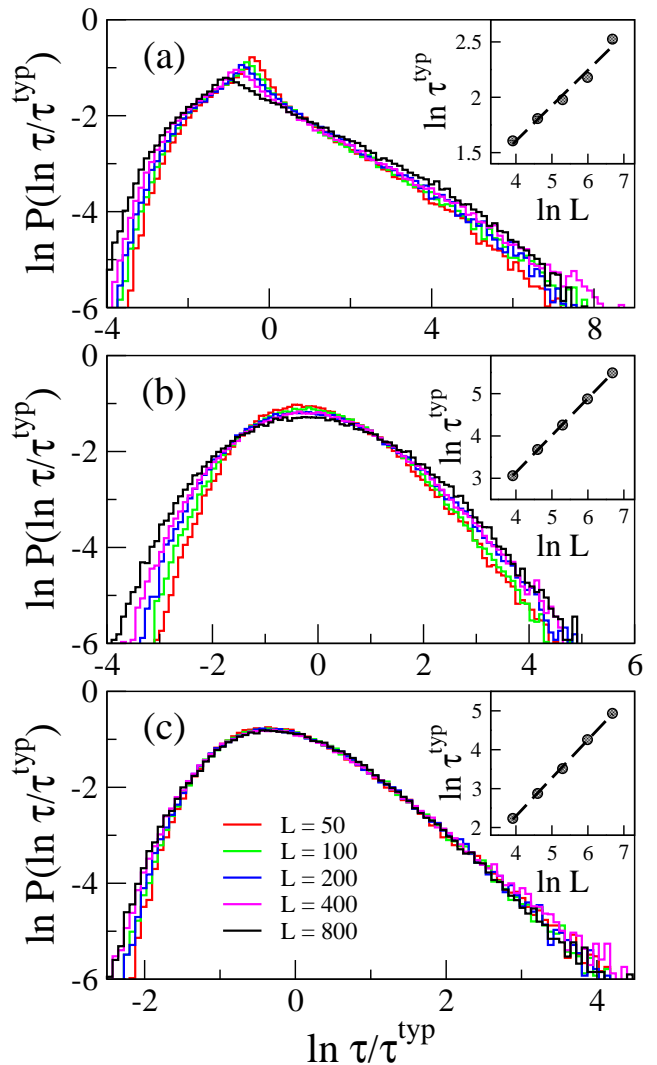


FIG. 3: (color online) $\ln \mathcal{P}(\ln \tau / \tau^{\text{typ}})$ as a function of $\ln \tau / \tau^{\text{typ}}$ for (a) $b = 0.1$, (b) $b = 1$, and (c) $b = 10$. In the insets the scaling $\tau^{\text{typ}} \propto L^{-\mu}$ is shown together with a linear fitting. $\tau^{\text{typ}} = \exp(\ln \tau)$. We found (a) $\mu = -0.318 \pm 0.027$, (b) $\mu = -0.874 \pm 0.006$, and (c) $\mu = -0.997 \pm 0.016$.

form distribution. Moreover, in this case, the expression⁹ $\mathcal{P}(\Phi) = 1/2\pi(\gamma + \sqrt{\gamma^2 - 1} \cos(\Phi))$ holds (not shown here); where $\gamma = (1 + |\langle S \rangle|^2) / (1 - |\langle S \rangle|^2)$ and $0 \leq \langle S \rangle \leq 1$.

IV. DISTRIBUTION OF DELAY TIMES AND RESONANCE WIDTHS

We first have to mention that moments of the the inverse Wigner delay time have been (numerically and analytically) shown to be related to the multifractal dimensions of eigenfunctions as^{8,9,10}

$$\langle \tau^{-q} \rangle = L^{-qD_{q+1}}, \quad (11)$$

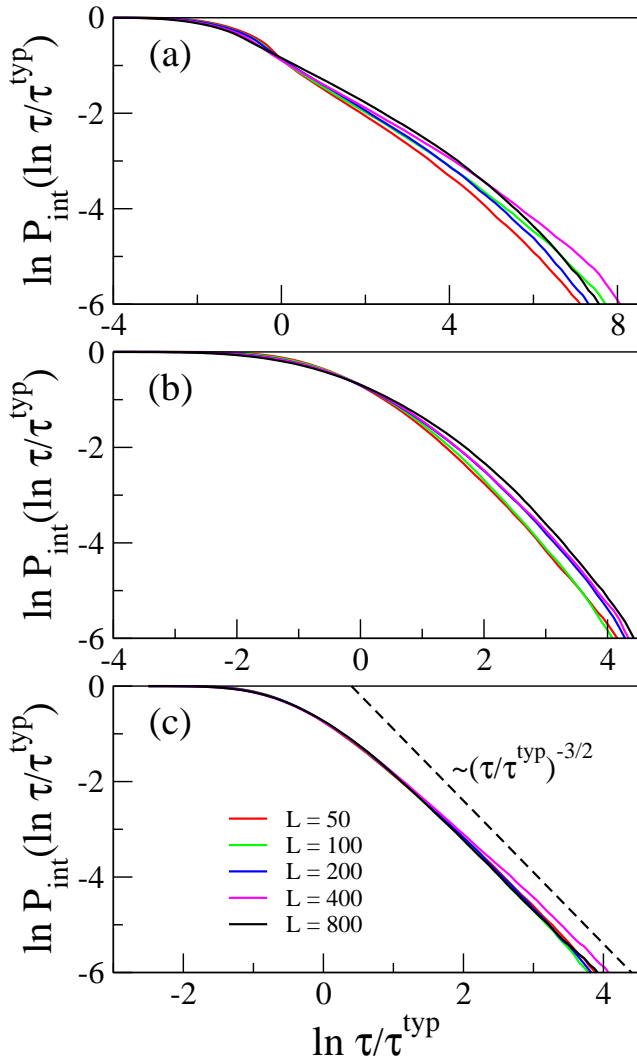


FIG. 4: (color online) $\ln \mathcal{P}_{\text{int}}(\ln \tau/\tau^{\text{typ}})$ as a function of $\ln \tau/\tau^{\text{typ}}$ for (a) $b = 0.1$, (b) $b = 1$, and (c) $b = 10$. The thin dashed line in (c) with slope $-3/2$ is plotted to guide the eye.

although the validity of this relation depends strongly whether the lead is attached to a site inside or at the border of the sample. However, in the case of the periodic PBRM model, studied here, all sites are *generic* and Eq. (11) holds well (not shown here).

Now, let us turn to the main results of our present investigation. We have looked at the distribution of Wigner delay times as well as that of the resonance widths a little bit differently, compared to previous works. First we tried to obtain a universal (i.e., L independent) form of the distribution function $\mathcal{P}(\ln \tau \Delta)$, where $\Delta \propto 1/\langle \tau \rangle \sim 1/L$. However, for small b the relation $\langle \tau \rangle \sim L$ does not hold and we have found a breakdown of the scaling of $\mathcal{P}(\ln \tau \Delta)$ with L , in contrast to the expectation according to Ref. 14.

Instead of $\langle \tau \rangle$ we decided to look at the typical value

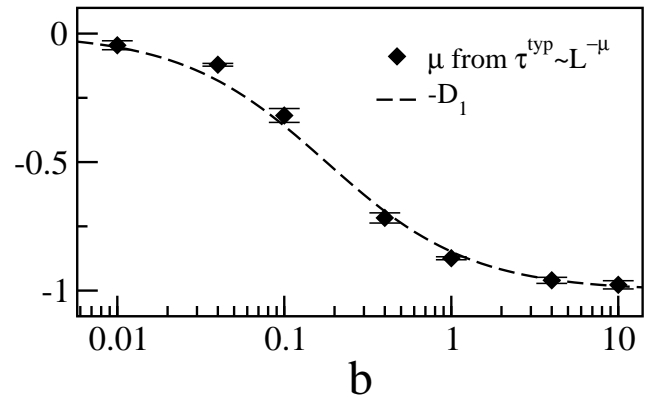


FIG. 5: μ as a function of b . μ is extracted from the scaling $\tau^{\text{typ}} \propto L^{-\mu}$, see Fig. 3. The dashed line is $-D_1$, where D_1 was obtained from Eq. (6) with $\sigma \approx 5.6$.

of τ : $\tau^{\text{typ}} = \exp \langle \ln \tau \rangle$. We found that $\mathcal{P}(\ln \tau/\tau^{\text{typ}})$ shows a good scaling with L and a tendency to a universal distribution (for each b) as $L \rightarrow \infty$, see Fig. 3. In Fig. 4 we also plot $\mathcal{P}_{\text{int}}(\ln \tau/\tau^{\text{typ}})$ to see the behavior of the tails of $\mathcal{P}(\ln \tau/\tau^{\text{typ}})$, where

$$\mathcal{P}_{\text{int}}(x) = \int_x^\infty \mathcal{P}(x') dx'. \quad (12)$$

Here, only for $b = 10$ we see a clear decay of the form $\mathcal{P}_{\text{int}}(\tau/\tau^{\text{typ}}) \sim (\tau/\tau^{\text{typ}})^{-3/2}$. Notice that the value of the exponent is the same as the one found in Ref. 14 for $\mathcal{P}_{\text{int}}(\tau/\langle \tau \rangle) \sim (\tau/\langle \tau \rangle)^{-3/2}$ in the case of the 3D Anderson model.

In view of Eq. (11) we may estimate the scaling behavior of τ^{typ} . Using a simple relation¹⁵ $\langle \ln \tau \rangle = \lim_{q \rightarrow 0} (\langle \tau^q \rangle - 1)/q$, we obtain

$$\tau^{\text{typ}} \propto L^{D_1}. \quad (13)$$

This is contrasted with the numerical results presented in Fig. 5 where we plot μ as a function of b . Here, μ is extracted from the scaling $\tau^{\text{typ}} \propto L^{-\mu}$ (see the insets in Fig. 3). The data agree well with Eq. (13).

In the case of resonance widths, we observe an excellent scaling of $\mathcal{P}(\ln \Gamma/\Gamma^{\text{typ}})$ for all values of b and the approach to a universal distribution (for each b) as $L \rightarrow \infty$, see Fig. 6. Here, $\Gamma^{\text{typ}} = \exp \langle \ln \Gamma \rangle$. Also, from Fig. 7 we observe that as $L \rightarrow \infty$, the integrated distribution function follows a power law decay $\mathcal{P}_{\text{int}}(\Gamma/\Gamma^{\text{typ}}) \sim (\Gamma/\Gamma^{\text{typ}})^{-1}$ for all values of b in complete agreement with Refs. 14 and 17.

Finally, in Fig. 8 we plot ν as a function of b where ν is extracted from the scaling $\Gamma^{\text{typ}} \propto L^{-\nu}$ (see the insets in Fig. 6). We found that ν is well approximated by $2 - D_2$.

Notice that in the limit $b \rightarrow \infty$, where $\nu \rightarrow 1$, we recover the full random matrix limit in which case we also have $\tau^{\text{typ}} \propto L \propto 1/\Delta$ and $\Gamma^{\text{typ}} \propto L^{-1} \propto \Delta$. This means, for instance, that as $b \rightarrow \infty$, $\mathcal{P}(\Gamma/\Gamma^{\text{typ}}) \rightarrow \mathcal{P}(\Gamma \Delta)$, where

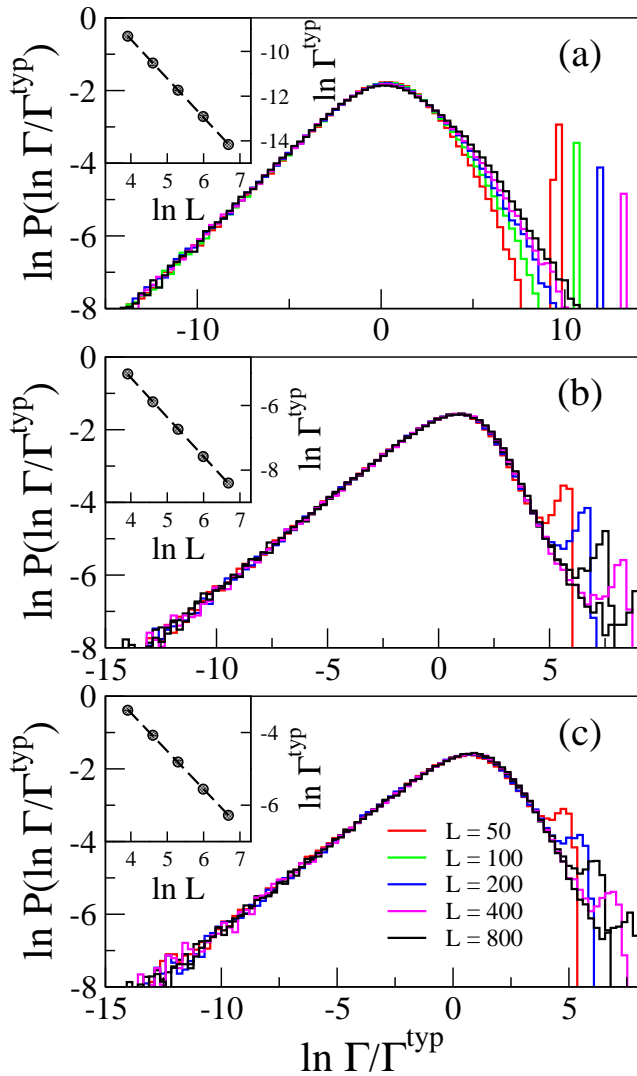


FIG. 6: (color online) $\ln \mathcal{P}(\ln \Gamma/\Gamma^{\text{typ}})$ as a function of $\ln \Gamma/\Gamma^{\text{typ}}$ for (a) $b = 0.1$, (b) $b = 1$, and (c) $b = 10$. In the insets the scaling $\Gamma^{\text{typ}} \propto L^{-\nu}$ is shown together with a linear fitting. $\Gamma^{\text{typ}} = \exp\langle \ln \Gamma \rangle$. We found (a) $\nu = 1.728 \pm 0.005$, (b) $\nu = 1.219 \pm 0.007$, and (c) $\nu = 1.048 \pm 0.008$.

the later scaling was found in Ref. 14 for the 3D Anderson model.

In Figs. 5 and 8 we see that the two quantities, τ^{typ} and Γ^{typ} , behave very similarly and in the limit of weak multifractality, $b \gg 1$, we nicely recover the features of the 3D Anderson transition.¹⁴ Moreover, this similarity calls for a simple scaling law

$$\tau^{\text{typ}} \propto L^{D_1} \quad \text{and} \quad \Gamma^{\text{typ}} \propto L^{-(2-D_2)}. \quad (14)$$

V. CONCLUSIONS

We have presented an analysis of the scattering properties of the PBRM model with one lead attached to it.

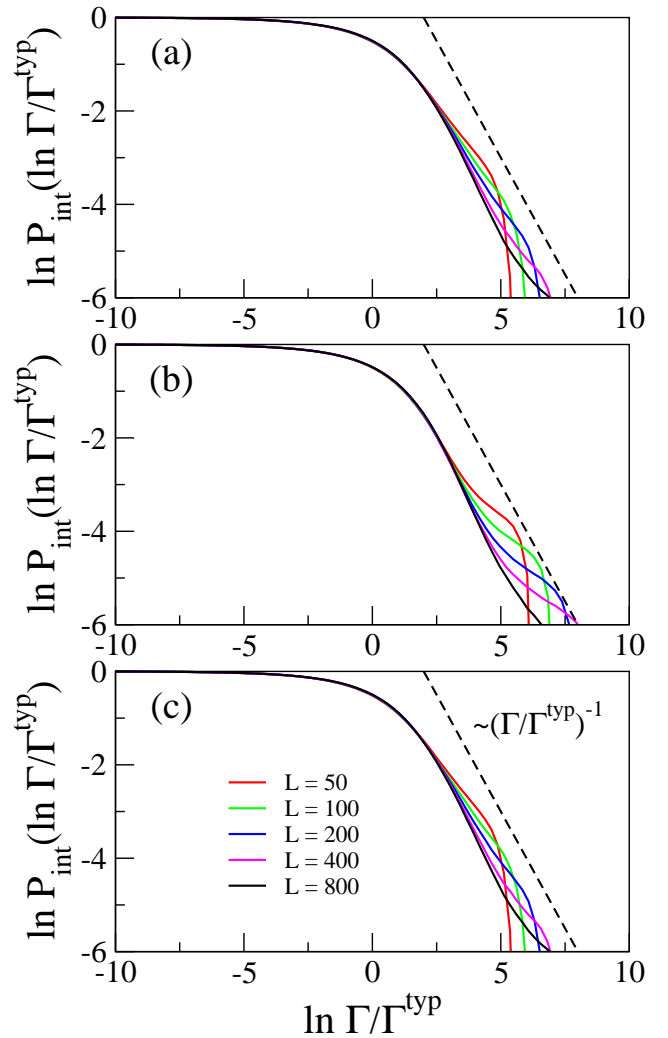


FIG. 7: (color online) $\ln \mathcal{P}_{\text{int}}(\ln \Gamma/\Gamma^{\text{typ}})$ as a function of $\ln \Gamma/\Gamma^{\text{typ}}$ for (a) $b = 0.1$, (b) $b = 1$, and (c) $b = 10$. The thin dashed lines with slope -1 are plotted to guide the eye.

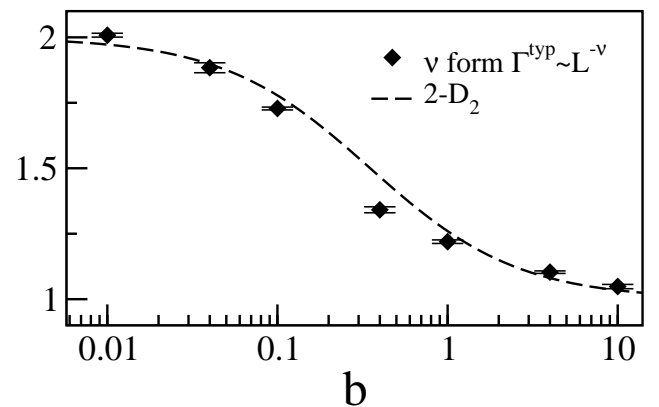


FIG. 8: ν as a function of b . ν is extracted from the scaling $\Gamma^{\text{typ}} \propto L^{-\nu}$, see Fig. 6. The dashed line is $2 - D_2$, where D_2 was obtained from Eq. (6) with $\sigma \approx 2.85$.

Especially, the system with large conductance (weak multifractality) shows remarkable correspondence with the properties of the standard 3D Anderson model at criticality. This is in accordance with earlier findings. We have also found a novel relation between the scaling of the Shannon entropy, described by D_1 , and the typical values of the Wigner delay times; as well as a relation between the scaling exponent of the participation number \mathcal{N}_2 , described by D_2 , and the resonance widths. On the other hand the decay of their integrated distribution functions behave just as they do for the Anderson transition in three dimensions.

Acknowledgments

One of the authors (I.V.) acknowledges enlightening discussions with D. V. Savin and Y. V. Fyodorov. This work was supported by the Alexander von Humboldt Foundation, the Hungarian Research Fund (OTKA) under T42981 and T46303, and the German-Israeli Foundation for Scientific Research and Development.

-
- ¹ P. W. Anderson, Phys. Rev. **109**, 1492 (1958); A. MacKinnon and B. Kramer, Rep. Prog. Phys. **56**, 1469 (1993); E. Abrahams, P. W. Anderson, D. C. Licciardello, and T. V. Ramakrishnan, Phys. Rev. Lett. **42**, 673 (1979); L. P. Gorkov, A. I. Larkin, and D. E. Khmel'nitskii, JETP Lett. **30** 228 (1979).
- ² *Mesoscopic Quantum Physics*, Proceedings of the Les Houches Session LXI, ed. E. Akkermans, G. Montambaux, J.-L. Pichard, and J. Zinn-Justin (North-Holland, Amsterdam) (1995).
- ³ B. L. Altshuler, V. E. Kravtsov, I. V. Lerner, in *Mesoscopic Phenomena in Solids*, ed. B. L. Altshuler, P. A. Lee, R. A. Webb (North Holland, Amsterdam), (1991).
- ⁴ B. I. Shklovskii, B. Shapiro, B. R. Sears, P. Lambrianides, and H. B. Shore, Phys. Rev. B **47**, 11487 (1993).
- ⁵ D. Braun, G. Montambaux, and M. Pascaud, Phys. Rev. Lett. **81**, 1062 (1998); V. E. Kravtsov and I. V. Lerner, *ibid.* **74**, 2563 (1995); B. L. Altshuler and B. I. Shklovskii, Zh. Eksp. Teor. Fiz. **91**, 220 (1986) [Sov. Phys. JETP **64**, 127 (1986)].
- ⁶ J. T. Chalker, I. V. Lerner, and R. A. Smith, Phys. Rev. Lett. **77**, 554 (1996); J.T. Chalker, V.E. Kravtsov, and I.V. Lerner, Pis'ma Zh. Éksp. Teor. Fiz. **64**, 355 (1996) [JETP Lett. **64**, 386 (1996)]; D. G. Polyakov, Phys. Rev. Lett. **81**, 4696 (1998).
- ⁷ J. T. Chalker and G. J. Daniell, Phys. Rev. Lett. **61**, 593 (1988); B. Huckestein and R. Klesse, Phys. Rev. B **59**, 9714 (1999).
- ⁸ J. A. Méndez-Bermúdez and T. Kottos, Phys. Rev. B **72**, 064108 (2005).
- ⁹ A. Ossipov and Y. V. Fyodorov, Phys. Rev. B **71**, 125133 (2005).
- ¹⁰ A. D. Mirlin, Y. V. Fyodorov, A. Mildenberger, F. Evers, Phys. Rev. Lett. **97**, 046803 (2006).
- ¹¹ A. Ossipov, T. Kottos and T. Geisel, Europhys. Lett. **62**, 719 (2003).
- ¹² Y. V. Fyodorov, JETP Letters **78**, 250 (2003).
- ¹³ C. Texier and A. Comtet, Phys. Rev. Lett., **82**, 4220 (1999); A. Ossipov, T. Kottos, and T. Geisel, Phys. Rev. B **61**, R11411 (2000).
- ¹⁴ T. Kottos, and M. Weiss, Phys. Rev. Lett. **89**, 056401 (2002).
- ¹⁵ We thank the referee for this suggestion.
- ¹⁶ F. Steinbach, A. Ossipov, T. Kottos, and T. Geisel, Phys. Rev. Lett. **85**, 4426, (2000).
- ¹⁷ M. Weiss, J. A. Méndez-Bermúdez, and T. Kottos, Phys. Rev. B **73**, 045103, (2006).
- ¹⁸ A. D. Mirlin, Y. V. Fyodorov, F.-M. Dittes, J. Quezada, and T. H. Seligman, Phys. Rev. E **54**, 3221 (1996).
- ¹⁹ A. D. Mirlin and F. Evers, Phys. Rev. B **62**, 7920 (2000).
- ²⁰ V. E. Kravtsov and K. A. Muttalib, Phys. Rev. Lett. **79**, 1913 (1997); V. E. Kravtsov and A. M. Tsel'el'ik, Phys. Rev. B **62**, 9888 (2000).
- ²¹ F. Evers and A. D. Mirlin, Phys. Rev. Lett. **84**, 3690 (2000); E. Cuevas, M. Ortuno, V. Gasparian, and A. Perez-Garrido, *ibid.* **88**, 016401 (2002).
- ²² I. Varga, Phys. Rev. B **66**, 094201 (2002); I. Varga and D. Braun, *ibid.* **61**, R11859 (2000).
- ²³ A. D. Mirlin, Phys. Rep. **326**, 259 (2000); Y. V. Fyodorov and A. D. Mirlin, Int. J. Mod. Phys. **8**, 3795 (1994); Y. V. Fyodorov and A. D. Mirlin, Phys. Rev. B **51**, 13403 (1995).
- ²⁴ P. Pradhan and S. Sridhar, Phys. Rev. Lett. **85**, 2360 (2000); H.-J. Stöckmann and J. Stein, *ibid.* **64**, 2215 (1990); S. Sridhar, *ibid.* **67**, 785 (1991); A. Kudrolli, V. Kidambi, and S. Sridhar, *ibid.* **75**, 822 (1995); H.-J. Stöckmann, M. Barth, U. Dörr, U. Kuhl, H. Schanze, Physica E **9**, 571 (2001).
- ²⁵ I. Varga and J. Pipek, Phys. Rev. E **68**, 026202 (2003).
- ²⁶ V. I. Falko and K. B. Efetov, Europhys. Lett. **32**, 627 (1995); Phys. Rev. B **52**, 17413 (1995).
- ²⁷ F. Wegner, Z. Phys. B **36**, 209 (1980); H. Aoki, J. Phys. C **16**, L205 (1983); M. Schreiber and H. Grussbach, Phys. Rev. Lett. **67**, 607 (1991); A. Mildenberger, F. Evers, and A. D. Mirlin, Phys. Rev. B **66**, 033109 (2002).
- ²⁸ H. G. E. Hentschel and I. Procaccia, Physica D **8**, 435 (1983); I. Varga and J. Pipek, J. Phys.: Condens. Matter **10**, 305 (1998).
- ²⁹ J. A. Méndez-Bermúdez, T. Kottos, and D. Cohen, Phys. Rev. E **73**, 036204 (2006)
- ³⁰ C. Mahaux and H. A. Weidenmüller, "Shell Model Approach in Nuclear Reactions", (North-Holland, Amsterdam), (1969); I. Rotter, Rep. Prog. Phys. **54**, 635 (1991); J. J. M. Verbaarschot, H. A. Weidenmüller, M. R. Zirnbauer, Phys. Rep. **129**, 367 (1985).
- ³¹ Y. V. Fyodorov, H.-J. Sommers, J. Math. Phys. **38** 1918 (1997); P. W. Brouwer, K. M. Frahm, C. W. J. Beenakker, Phys. Rev. Lett. **78**, 4737 (1997); H.-J. Sommers, D. V. Savin, V. V. Sokolov, *ibid.* **87**, 094101 (2001).
- ³² I. L. Aleiner, P. W. Brouwer, L. I. Glazman, Phys. Rep. **358**, 309 (2002); Y. Alhassid, Rev.Mod.Phys. **72**, 895 (2000).